Transmission of correlated electrons through sharp domain walls in magnetic nanowires: A renormalization group approach

M. A. N. Araújo,[1,2,*] V. K. Dugaev,[2,3,4] V. R. Vieira,[2] J. Berakdar,[5] and J. Barnaś[6,7]

[1]*Department of Physics, Massachusetts Institute of Technology, Cambridge, Massachusetts 02139, USA*

[2]*CFIF and Departamento de Física, Instituto Superior Técnico, Av. Rovisco Pais, 1049-001 Lisbon, Portugal*

[3]*Frantsevich Institute for Problems of Materials Science, National Academy of Sciences of Ukraine, Vilde 5, 58001 Chernovtsy, Ukraine*

[4]*Department of Mathematics and Applied Physics, University of Technology, Al. Powstancow Warszawy 6, 35-959 Rzeszow, Poland*

[5]*Max-Planck Institut für Mikrostrukturphysik, Weinberg 2, 06120 Halle, Germany*

[6]*Department of Physics, Adam Mickiewicz University, Umultowska 85, 61-614 Poznań, Poland*

[7]*Institute of Molecular Physics, Polish Academy of Sciences, Smoluchowskiego 17, 60-179 Poznań, Poland*

(Received 6 October 2006; revised manuscript received 6 November 2006; published 26 December 2006)

The transmission of correlated electrons through a domain wall in a ferromagnetic one-dimensional system is studied theoretically in the limit of a domain wall width smaller or comparable to the electron Fermi wavelength. The domain wall gives rise to both potential and spin-dependent scattering of the charge carriers. Using a "poor man's" renormalization group approach for the electron-electron interactions, we obtain the low temperature behavior of the reflection and transmission coefficients. The results show that the low-temperature conductance is governed by the electron correlations, which may suppress charge transport without suppressing spin current. The results may account for a huge magnetoresistance associated with a domain wall in ballistic nanocontacts.

DOI: 10.1103/PhysRevB.74.224429 PACS number(s): 75.70.Cn, 71.10.Pm, 73.63.Nm, 75.75.+a

I. INTRODUCTION

Domain walls (DWs), i.e., the boundaries separating different domains of homogeneous magnetizations,[1] are recently a subject of extensive theoretical and experimental investigations. This renewed interest in DWs is stimulated by their possible applications in magnetic logic elements and other nanoelectronics and spintronics devices. Two effects associated with DWs are of particular interest. The first one is the way a DW affects electronic transport, i.e., the associated magnetoresistance. The crucial point here is that the influence of a single DW on the resistance can be controlled by an external magnetic field.[2,3] The second effect concerns the influence of electric current on the DW behavior (DW motion, magnetic switching),[4] which allows controlling of DWs by means of an electric field.

Recent advances in experimental techniques have made possible the determination of the resistance of a single DW in submicron structured samples.[2,5–11] The results on the single domain resistance are different in magnitude and sometimes differ also in the sign. In the case where the DW width is large on the scale set by the Fermi wavelength, λ_F, of the carriers, the theory of the DW contribution to electrical resistance is well established.[12–17] The spin of the electron moving across the wall changes its orientation quasiadiabatically (or even adiabatically for very thick DWs). However, the DWs formed at nanoconstrictions may be atomically sharp[18–21] and the spin of an electron crossing the wall does not change quasiadiabatically. Accordingly, a completely different approach to the transport theory through DWs is required. This is particularly true for ferromagnetic semiconductors which are considered to be most promising for spintronic applications.[22] Indeed, recent experiments on magnetic nanostructures and nanowires indicate that the presence of DWs may result in a magnetoresistance (MR) as large as several hundreds[8,23] or even thousands[24,25] of percents, as opposed to the case of thick on scale of λ_F (or adiabatic) DWs in bulk metallic ferromagnets. In the ballistic regime, the theoretical treatments towards explaining this effect[26–31] rely on the assumption that the DW is sharp enough to be treated as a spin-dependent scatterer for the charge carriers. The success of these theories in explaining the extraordinary large MR is moderate, in particular for metallic ferromagnets such as Ni where some features of the physics governing the behavior of MR are still unclear.[32]

Another feature of the DWs created at nanoconstrictions is their small lateral size (cross section of the constriction). This small size limits the number of quantum channels active in transport to a few ones or even to a single one. Consequently, the constriction behaves as a one- or quasi-one-dimensional system. In such a case, the role of electron-electron interactions may be crucial[33] for understanding the behavior and basic transport characteristics of the DWs formed at nanoconstrictions. It is well established that electronic correlations in a one-channel wire result in a non-Fermi-liquid behavior—thus forming a Luttinger liquid.[34,35] It is also known that an impurity present in the 1D Luttinger liquid suppresses the linear conductivity, which vanishes even for a weak impurity scattering potential.[36,37] This can be traced back to a vanishing density of states at the Fermi level. At finite applied voltages the transport through the wire does not vanish due to the nonlinearity of the current-voltage characteristics.[36] Since a sharp domain wall acts in a one-channel wire as a localized spin-dependent scattering center, one can expect a strong influence of electron correlations on the MR at low temperatures.

To confirm this theoretically one could use bosonization techniques.[38,39] However, we will follow another route based on the "poor man's" renormalization method.[40–42] In our case, the DW scatters both the charge and spin of the carriers. As shown below, our scheme allows us to obtain results for the renormalized transmission and reflection coefficients in terms of the uncorrelated spin-dependent ones (i.e., in terms of the reflection and transmission coefficients of the wall in the absence of electron-electron interactions). The uncorrelated quantities can be obtained from other schemes, such as the Hartree-Fock or density-functional theory (within local density approximation) and then used as an input in our results to obtain renormalized transmission through the DW. Hence, our approach—in combination with numerical (effective single particle) methods—offers a new possibility to understand the material-dependent MR associated with a DW creation (destruction), and possibly to resolve some controversy concerning huge magnetoresistance in some ballistic nanocontacts.

The paper is organized as follows. In Sec. II we introduce the problem and the noninteracting scattering states for a sharp domain wall. In Sec. III we use perturbation theory in the electron-electron interaction to calculate corrections to the scattering amplitudes. We obtain the renormalization group differential equations for the scattering amplitudes. In Sec. IV we describe the zero temperature fixed points predicted by the scaling equations and the power-law behavior of the reflection and transmission coefficients of the DW as $T\to 0$. In Sec. V we discuss the relevance of our findings to realistic physical systems and summarize our results.

II. MODEL

We consider a magnetized system with electrons being constrained to move in one dimension while being exchange-coupled locally to the space varying magnetization, $\mathbf{M}(\mathbf{r})$. The wire itself defines the easy (z) axis, and a domain wall centered at $z=0$ separates two regions with opposite magnetizations, $M_z(z\to\pm\infty)=\pm M_0$. Assuming $\mathbf{M}(\mathbf{r})$ to lie in the xz plane, and the domain wall to be thinner than the Fermi wavelength, we write the single-particle Hamiltonian as

$$\hat{H}_0 = -\frac{\hbar^2}{2m}\frac{d^2}{dz^2} + \hbar V\delta(z) + JM_z(z)\hat{\sigma}_z + \hbar\lambda\,\delta(z)\hat{\sigma}_x, \quad (1)$$

where the term $\hbar\lambda\,\delta(z)\hat{\sigma}_x$ describes spin scattering produced by the $M_x(z)$ component,[43]

$$\lambda = \frac{J}{\hbar}\int_{-\infty}^{\infty} M_x(z)dz,$$

and V is a potential scattering term. Single electron wave functions are spinors with components $\chi_\sigma(z)$ satisfying the condition

$$-\frac{\hbar}{2m}\left(\frac{\partial}{\partial z}\chi_\sigma(0^+) - \frac{\partial}{\partial z}\chi_\sigma(0^-)\right) + V\chi_\sigma(0) - \lambda\chi_{-\sigma}(0) = 0. \quad (2)$$

The electron's wave vector in each domain is related to the energy E by

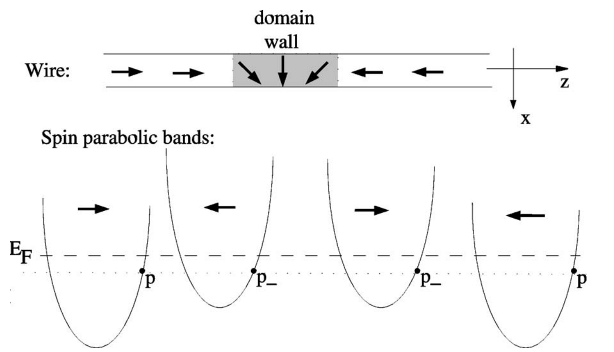

FIG. 1. Schematic of a domain wall and the relevant electron spin bands. States $\psi_{p\uparrow}$ and $\psi_{p_-\downarrow}$ have the same energy.

$$k = \sqrt{\frac{2m}{\hbar^2}(E \pm JM_0)}. \quad (3)$$

The electron gas in the negative semiaxis $(z<0)$ is predominantly $\uparrow$-spin. An electron incident from the left with the momentum k and spin $\uparrow$ (or $\downarrow$) can be transmitted to the positive semiaxis while preserving its spin, but the energy conservation requires the momentum to change from k to k_- (or k_+) defined by

$$k_\pm = \sqrt{k^2 \pm \frac{4m}{\hbar^2}JM_0}. \quad (4)$$

If the transmission occurs with spin reversal, the momentum k is not changed. (See Fig. 1.)

We label the states through the incident wave, so that

$$\psi_{k,\uparrow}(z) = \begin{pmatrix} e^{ikz} + r_\uparrow(k)e^{-ikz} \\ r'_\uparrow(k)e^{-ik_-z} \end{pmatrix}, \quad z<0 \quad (5)$$

describes a scattering state with a wave incident from $z=-\infty$ with spin $\uparrow$ and momentum $k>0$. Reflection amplitudes of a spin σ electron with or without spin reversal are denoted by r'_σ and r_σ, respectively. The same convention applies to the transmission amplitudes t'_σ, t_σ. The transmitted wave corresponding to Eq. (5) is

$$\psi_{k,\uparrow}(z) = \begin{pmatrix} t_\uparrow(k)e^{ik_-z} \\ t'_\uparrow(k)e^{ikz} \end{pmatrix}, \quad z>0 \quad (6)$$

and the scattering amplitudes are given by

$$t_\uparrow(k) = \frac{2(v+v_-+2iV)v}{(v+v_-+2iV)^2+4\lambda^2} = r_\uparrow(k)+1, \quad (7)$$

$$t'_\uparrow(k) = \frac{4i\lambda v}{(v+v_-+2iV)^2+4\lambda^2} = r'_\uparrow(k), \quad (8)$$

where we have defined the velocities $v_{(\pm)}=\hbar k_{(\pm)}/m$.

The scattering state corresponding to a wave incident from the left-hand side with $\downarrow$-spin is

$$\psi_{k,\downarrow}(z<0)=\begin{pmatrix} r'_\downarrow(k)e^{-ik_+z} \\ e^{ikz}+r_\downarrow(k)e^{-ikz}\end{pmatrix},$$

$$\psi_{k,\downarrow}(z>0)=\begin{pmatrix} t'_\downarrow(k)e^{ikz} \\ t_\downarrow(k)e^{ik_+z}\end{pmatrix}, \tag{9}$$

and the corresponding amplitudes are

$$t_\downarrow(k)=\frac{2(v+v_++2iV)v}{(v+v_++2iV)^2+4\lambda^2}=r_\downarrow(k)+1, \tag{10}$$

$$t'_\downarrow(k)=\frac{4i\lambda v}{(v+v_++2iV)^2+4\lambda^2}=r'_\downarrow(k). \tag{11}$$

The expressions for the scattering states corresponding to the waves incident from $+\infty$ are

$$\psi_{-k,\uparrow}(z<0)=\begin{pmatrix} t_\downarrow(k)e^{-ik_+z} \\ t'_\downarrow(k)e^{-ikz}\end{pmatrix},$$

$$\psi_{-k,\uparrow}(z>0)=\begin{pmatrix} e^{-ikz}+r_\downarrow(k)e^{ikz} \\ r'_\downarrow(k)e^{ik_+z}\end{pmatrix} \tag{12}$$

and

$$\psi_{-k,\downarrow}(z<0)=\begin{pmatrix} t'_\uparrow(k)e^{-ikz} \\ t_\uparrow(k)e^{-ik_-z}\end{pmatrix},$$

$$\psi_{-k,\downarrow}(z>0)=\begin{pmatrix} r'_\uparrow(k)e^{ik_-z} \\ e^{-ikz}+r_\uparrow(k)e^{ikz}\end{pmatrix}, \tag{13}$$

where we consider $k>0$. We shall henceforth denote by $\epsilon(\pm p,\uparrow)$ the eigenenergy of a scattering state with momentum $+p$ (or $-p$) incident from the left-hand side (or right-hand side). The scattering amplitudes satisfy some general relations that can be found from a generalization of the Wronskian theorem[44] to spinor wave functions. We provide such relations in Appendix A.

In order to deal with the electron interactions, it is convenient to rewrite the scattering states in second quantized form, making use of right ($\hat{a}_{q\sigma}$) and left ($\hat{b}_{q\sigma}$) moving plane-wave states.

The operators for the scattering states with electrons incident from the left ($\hat{c}_{k,\sigma}$) are

$$\hat{c}_{k,\sigma}=\int_{-\infty}^{\infty}\frac{dq}{2\pi}\Bigg[\left(\frac{-i}{q-k-i0}+\frac{it^*_\sigma(k)}{q-k_{-\sigma}+i0}\right)\hat{a}_{q\sigma} - \frac{ir^*_\sigma(k)}{q+k-i0}\hat{b}_{q\sigma}+\frac{it'^*_\sigma(k)}{q-k+i0}\hat{a}_{q,-\sigma}-\frac{ir'^*_\sigma(k)}{q+k_{-\sigma}-i0}\hat{b}_{q,-\sigma}\Bigg], \tag{14}$$

and the operators for scattering states with electrons incident from the right ($\hat{d}_{k,\sigma}$) are

$$\hat{d}_{k,\sigma}=\int_{-\infty}^{\infty}\frac{dq}{2\pi}\Bigg[\left(\frac{i}{q+k+i0}-\frac{it^*_{-\sigma}(k)}{q+k_\sigma-i0}\right)\hat{b}_{q\sigma}+\frac{ir^*_{-\sigma}(k)}{q-k+i0}\hat{a}_{q\sigma} - \frac{it'^*_{-\sigma}(k)}{q+k-i0}\hat{b}_{q,-\sigma}+\frac{ir'^*_{-\sigma}(k)}{q-k_\sigma+i0}\hat{a}_{q,-\sigma}\Bigg], \tag{15}$$

where 0 denotes a positive infinitesimal and the k subscript $\sigma=\pm 1$. By inverting these equations, we obtain the plane wave operators as linear combinations of the scattering state operators,

$$\hat{a}_{p,\sigma}=\int_{-\infty}^{\infty}\frac{dk}{2\pi i}\Bigg(\frac{\hat{c}_{k,\sigma}}{k-p-i0}-\frac{t_{-\sigma}(k)\hat{c}_{k_+,\sigma}}{k-p+i0}-\frac{t'_{-\sigma}(k)\hat{c}_{k,-\sigma}}{k-p+i0} - \frac{r_{-\sigma}(k)\hat{d}_{k,\sigma}}{k-p+i0}-\frac{r'_{-\sigma}(k)\hat{d}_{k_+,-\sigma}}{k-p+i0}\Bigg), \tag{16}$$

$$\hat{b}_{-p,\sigma}=\int_{-\infty}^{\infty}\frac{dk}{2\pi i}\Bigg(\frac{\hat{d}_{k,\sigma}}{k-p-i0}-\frac{t_{\sigma}(k)\hat{d}_{k_-,\sigma}}{k-p+i0}-\frac{t'_{\sigma}(k)\hat{d}_{k,-\sigma}}{k-p+i0} - \frac{r_{\sigma}(k)\hat{c}_{k,\sigma}}{k-p+i0}-\frac{r'_{\sigma}(k)\hat{c}_{k_-,-\sigma}}{k-p+i0}\Bigg). \tag{17}$$

The electron interactions are introduced in the Hamiltonian through the term

$$\hat{H}_{\rm int}=g_{1,\alpha,\beta}\int\frac{dk_1dq}{(2\pi)^2}\hat{a}^\dagger_{k_1,\alpha}\hat{b}^\dagger_{k_2,\beta}\hat{a}_{k_2+q,\beta}\hat{b}_{k_1-q,\alpha} + g_{2,\alpha,\beta}\int\frac{dk_1dq}{(2\pi)^2}\hat{a}^\dagger_{k_1,\alpha}\hat{b}^\dagger_{k_2,\beta}\hat{b}_{k_2+q,\beta}\hat{a}_{k_1-q,\alpha}. \tag{18}$$

The coupling constants g_1 and g_2 describe back and forward scattering processes between opposite moving electrons, respectively. The greek letters denote here the spin indices, and the summation over repeated indices is implied. Because the Fermi momentum depends on spin, we allow for the dependence of g on the spins of the interacting particles. We therefore distinguish between $g_{1\uparrow}$, $g_{1\downarrow}$, $g_{1\perp}$, and $g_{2\uparrow}$, $g_{2\downarrow}$, $g_{2\perp}$. The forward scattering process between particles which move in the same direction will not affect the transmission amplitudes, although it will renormalize the Fermi velocity.[40] This effect is equivalent to an effective mass renormalization and the electrons with different spin orientations may turn out to have different effective masses, in which case our calculations remain valid, as shown in Appendix B.

III. SCALING EQUATIONS

The corrections to the transmission amplitudes will be calculated to first order in the perturbation $\hat{H}_{\rm int}$. It has been shown in Ref. 40 that the corrections diverge logarithmically near the Fermi level. These divergences will later be dealt with in a poor man's renormalization procedure.

Let us consider the Matsubara propagator,

$$\mathcal{G}(\tau) = -\langle T_\tau e^{-\int \hat{H}_{\text{int}}(\tau')d\tau'} \hat{a}_{p,\uparrow}(\tau)\hat{c}^\dagger_{p',\uparrow}\rangle_0, \tag{19}$$

where $\langle\cdots\rangle_0$ denotes the average in the noninteracting Fermi sea. The propagator for noninteracting electrons is then given by

$$\mathcal{G}^{(0)}(i\omega) = \frac{1}{i\omega - \epsilon(p',\uparrow)}\left(\frac{i}{p-p'+i0} - \frac{it_\uparrow(p')}{p-p'_- - i0}\right). \tag{20}$$

The transmission amplitude appears associated with the denominator $p-p'_- - i0$ which, for the variable p, gives a pole in the upper half-plane. The meaning of this pole is that the transmitted particle is a right mover in the $z>0$ half-axis. Our strategy is to calculate the first order correction term (in $\hat{H}_{\text{int}}$) to $\mathcal{G}$, which will have the same form as the second term in (20), so that the amplitude correction, $\delta t_\uparrow(p')$, can be read off from the result. We now explain the procedure in some detail.

We begin by considering the first order expansion for $\mathcal{G}$ in the coupling $g_{1\uparrow}$. For simplicity, we shall henceforth omit the subscript "0" in the brackets, since we will be dealing with the noninteracting Fermi sea, unless otherwise stated. From Wick's theorem we get the first order correction to the propagator in Eq. (20) as

$$\begin{aligned}\mathcal{G}^{(1)}(\tau) = g_{1\uparrow}[&\langle\hat{a}_{p,\uparrow}(\tau)\hat{b}^\dagger_{k_2,\uparrow}(\tau')\rangle\langle\hat{a}^\dagger_{k_1,\uparrow}(\tau')\hat{b}_{k_1-q,\uparrow}(\tau')\rangle \\ &\times\langle\hat{a}_{k_2+q,\uparrow}(\tau')\hat{c}^\dagger_{p',\uparrow}\rangle + \langle\hat{a}_{p,\uparrow}(\tau)\hat{a}^\dagger_{k_1,\uparrow}(\tau')\rangle \\ &\times\langle\hat{b}^\dagger_{k_2,\uparrow}(\tau')\hat{a}_{k_2+q,\uparrow}(\tau')\rangle\langle\hat{b}_{k_1-q,\uparrow}(\tau')\hat{c}^\dagger_{p',\uparrow}\rangle],\end{aligned} \tag{21}$$

where the internal momenta $k_{1(2)}$, q and time τ' are to be integrated over and the time ordering T_τ is implicit. There are also two other Wick paired terms at instant τ' of the form $\langle\hat{a}^\dagger(\tau')\hat{a}(\tau')\rangle$ and $\langle\hat{b}^\dagger(\tau')\hat{b}(\tau')\rangle$. We have omitted these terms in Eq. (21) because they will not be logarithmically divergent: the divergences arise from electron reflection by the Friedel oscillations in the Fermi sea.[40] Such reflection processes appear in Eq. (21) through $\langle\hat{b}^\dagger(\tau')\hat{a}(\tau')\rangle$ and $\langle\hat{a}^\dagger(\tau')\hat{b}(\tau')\rangle$.

To calculate $\langle\hat{a}^\dagger_{k_1,\uparrow}\hat{b}_{k_1-q,\uparrow}\rangle$ we make use of the expression (17) for $\hat{b}_{k_1-q,\uparrow}$. The contour integration over k_1 eliminates the terms containing poles in the same half-plane. Fermi sea averages, such as $\langle\hat{a}^\dagger_{k_1,\uparrow}\hat{c}_{k,\uparrow}\rangle$ and $\langle\hat{a}^\dagger_{k_1,\uparrow}\hat{d}_{k,\uparrow}\rangle$, can be calculated in the same way as in Eq. (20). The result is

$$\begin{aligned}&\int_{-\infty}^{\infty}\frac{dk_1}{2\pi}\langle\hat{a}^\dagger_{k_1,\uparrow}\hat{b}_{k_1-q,\uparrow}\rangle \\ &\quad = \int_{-\infty}^{\infty}\frac{dQ}{2\pi i}\left(\frac{f(-Q\uparrow)r^*_\downarrow(Q)}{2Q-q-i0} - \frac{f(Q\uparrow)r^*_\uparrow(Q)}{2Q-q+i0}\right),\end{aligned} \tag{22}$$

where $f(\pm Q\uparrow)$ denotes the Fermi occupation number of the state $\psi_{\pm Q,\uparrow}$. In order to calculate the propagator $-\langle\hat{T}_\tau a_{p,\uparrow}(\tau)\hat{b}^\dagger_{k_2,\uparrow}\rangle$ we again expand $\hat{b}^\dagger_{k_2,\uparrow}$ using Eq. (17), and then with help of Eq. (A7) we obtain

$$\begin{aligned}&-\int_0^{1/T} d\tau e^{i\omega\tau}\langle\hat{T}_\tau a_{p,\uparrow}(\tau)\hat{b}^\dagger_{-p',\uparrow}\rangle \\ &\quad = \int_{-\infty}^{\infty}\frac{dQ}{2\pi}\left(\frac{1}{i\omega-\epsilon(-Q\uparrow)}\frac{1}{Q-p'+i0}\frac{r_\downarrow(Q)}{p-Q-i0}\right. \\ &\quad\quad \left. + \frac{1}{i\omega-\epsilon(Q\uparrow)}\frac{1}{Q-p'-i0}\frac{r^*_\uparrow(Q)}{p-Q+i0}\right).\end{aligned} \tag{23}$$

The presence of two different energy poles can be understood from the fact that $\hat{a}_{q\sigma}$ (or $\hat{b}_{q\sigma}$) represents a plane wave running over the entire z axis and its energy cannot be the same on both sides of the domain wall because of the energy dependence on spin.

Using Eqs. (22) and (23) we can calculate the first term in Eq. (21) as

$$\begin{aligned}&\langle\hat{a}_{p,\uparrow}(\tau)\hat{b}^\dagger_{k_2,\uparrow}(\tau')\rangle\langle\hat{a}^\dagger_{k_1,\uparrow}(\tau')\hat{b}_{k_1-q,\uparrow}(\tau')\rangle\langle\hat{a}_{k_2+q,\uparrow}(\tau')\hat{c}^\dagger_{p',\uparrow}\rangle \\ &\quad = \frac{1}{i\omega-\epsilon(p'\uparrow)}\int\frac{dQ_1dQ_2}{(2\pi i)^2}\frac{1}{i\omega-\epsilon(-Q_2\uparrow)} \\ &\quad\quad\times\frac{r_\downarrow(Q_2)r^*_\downarrow(Q_1)t^*_\uparrow(p')f(-Q_1\uparrow)}{(p-Q_2-i0)(2Q_1-p'_- -Q_2-i0)}.\end{aligned} \tag{24}$$

The analytic continuation of the Green's function frequency, $i\omega\to\omega+i0$, gives the retarded Green's function. the frequency denominator $[i\omega-\epsilon(-Q_2\uparrow)]^{-1}$ yields a principal Cauchy part plus a delta function part. The latter isolates the energy pole at $\epsilon(-Q_2\uparrow)=\omega$ and we choose $\omega=\epsilon(p'\uparrow)\Rightarrow Q_2=p'_-$. We shall only retain this delta function part. Therefore, we set $Q_2=p'_-$ in the integrand and, by comparing with (20), we conclude that the contribution of the first perturbative term in Eq. (21) to the transmission amplitude is given by

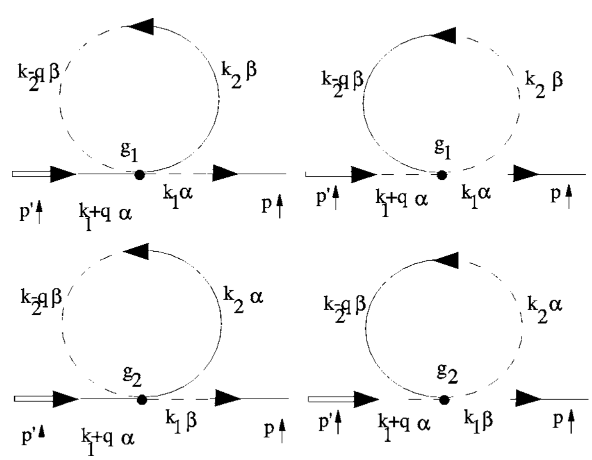

FIG. 2. Feynmam diagrams for the first order contribution $\mathcal{G}^{(1)}$ to the propagator (19). The scattering state is represented by a double line, the $\hat{a}$ ($\hat{b}$) particle is represented by a continuous (dashed) line. The loop represents the Hartree-Fock potential of the Fermi sea. The scattered electron exchanges momentum q with the Fermi sea.

$$\delta t_{\uparrow}(p') = - \frac{g_{1\uparrow}}{hv_{F-}} \int \frac{dQ}{2\pi} \frac{f(-Q\uparrow)}{2Q - 2p'_-} r_{\downarrow}(p'_-) r^*_{\downarrow}(Q) t^*_{\uparrow}(p'), \tag{25}$$

where v_{F-} now denotes the Fermi velocity corresponding to the minority spin Fermi momentum k_{F-}. A logarithmic divergence appears as $p' \to k_{F-}$.

The above discussion describes the calculation method. We now need to calculate all the first order terms in the interactions $g_{1\alpha\beta}$ and $g_{2\alpha\beta}$. The diagrammatic representation of $\mathcal{G}^{(1)}$ is shown in Fig. 2. The horizontal lines represent the electron being scattered by the Hartree-Fock potential of the Fermi sea (of scattering states). Consider, for instance, the upper left diagram: an electron, initially in state $c_{p',\uparrow}$ close to the Fermi level, passes through the barrier as a right mover ($\hat{a}$ particle) and then interacts with the Fermi sea (on the positive z semiaxis). The electron is reflected (from $\hat{a}$ to $\hat{b}$ particle) while exchanging momentum q with the Fermi sea. Finally, it is reflected by the barrier again, becoming a spin-up right mover with momentum p. A logarithmic divergence occurs if the polarized Fermi sea can provide exactly the momentum that is required to keep the electron always near the Fermi level during the intermediate virtual steps. Concerning the spin dependence of the interaction parameters, we distinguish between $g_{1\uparrow}$, $g_{2\uparrow}$, which describe interaction between spin majority particles (that is spin-$\uparrow$ on the right and spin-$\downarrow$ on the left of the barrier) and $g_{1\downarrow}$, $g_{2\downarrow}$, which describe interaction between spin minority particles (that is spin-$\downarrow$ on the right and spin-$\uparrow$ on the left of the barrier). We use $g_{1\perp}$, $g_{2\perp}$ to denote interaction between particles with opposite spins. According to the physical interpretation of the Feynman diagrams just given above, we always know on which side of the barrier the interaction with the Fermi sea (closed loop in the diagram) is taking place.

It can be seen that the $g_{1\perp}$ terms are proportional to $\ln|k_{F+}-k_{F-}|$, so they do not diverge. The logarithmic divergence would be restored in a spin degenerate system ($k_{F+} = k_{F-}$). This can be understood from the diagrams in Fig. 2 as follows: the electron with spin α is reflected by a polarized Fermi sea with spin $-\alpha$. The momentum provided by the Fermi sea is $2k_{F-\alpha}$, while the momentum required by the electron is $2k_{F\alpha}$. The $g_{2\perp}$ terms produce logarithmic divergences that would not exist in the absence of spin-flip scattering ($t' = r' = 0$). Introducing the Fermi level velocities $v_{F\pm}$ for majority or minority spin particles, we write the diverging contributions to $\delta t_{\uparrow}(p')$ as

$$\begin{aligned}
\delta t_{\uparrow}(p') = & \int^{K_{F-}} \frac{dQ}{4hv_{F-}} \frac{(g_{2\downarrow} - g_{1\downarrow}) r_{\downarrow}(p'_-) r^*_{\downarrow}(Q) t_{\uparrow}(p')}{Q - p'_-} + \int^{K_{F+}} \frac{dQ}{4hv_{F+}} \frac{(g_{2\uparrow} - g_{1\uparrow}) t_{\uparrow}(p') r^*_{\uparrow}(Q) r_{\uparrow}(p')}{Q - p'} \\
& + \int^{K_{F+}} \frac{dQ}{4hv_{F+}} \frac{(g_{2\uparrow} - g_{1\uparrow}) r'_{\uparrow}(p') r^*_{\uparrow}(Q) t'_{\uparrow}(p')}{Q - p'} + \int^{K_{F-}} \frac{dQ}{4hv_{F-}} \frac{(g_{2\downarrow} - g_{1\downarrow}) t'_{\downarrow}(p' -) r^*_{\downarrow}(Q) r'_{\uparrow}(p')}{Q - p'_-} \\
& + \int^{K_{F+}} \frac{dQ}{2hv_{F+}} \frac{g_{2\perp} r'^*_{\uparrow}(Q) t_{\uparrow}(p') r'_{\uparrow}(p')}{Q + Q_- - p' - p'_-} + \int^{K_{F+}} \frac{dQ}{2hv_{F-}} \frac{g_{2\perp} r'^*_{\uparrow}(Q) t'_{\downarrow}(p'_-) r_{\uparrow}(p')}{Q + Q_- - p' - p'_-} + \int^{K_{F+}} \frac{dQ}{2hv_{F+}} \frac{g_{2\perp} r'^*_{\uparrow}(Q) r'_{\uparrow}(p') t_{\uparrow}(p')}{Q + Q_- - p' - p'_-} \\
& + \int^{K_{F-}} \frac{dQ}{2hv_{F-}} \frac{g_{2\perp} r'^*_{\downarrow}(Q) r_{\downarrow}(p'_-) t'_{\uparrow}(p')}{Q + Q_+ - p' - p'_-},
\end{aligned} \tag{26}$$

where $Q_\pm$ is related to Q as in Eq. (4). In order to apply the poor man's renormalization method, it is preferable to transform the momentum integrations in Eq. (26) into energy integrals. In order to do this, we linearize the spectrum near the Fermi level as

$$\hbar v_{F+}(Q - K_{F+}) = \hbar v_{F-}(Q_- - K_{F-}) \equiv \epsilon, \tag{27}$$

$$\hbar v_{F+}(p' - K_{F+}) = \hbar v_{F-}(p'_- - K_{F-}) \equiv \epsilon', \tag{28}$$

where energy of the scattered electron is ϵ' and the energies $\epsilon(\epsilon') < 0$ are measured with respect to the Fermi level. The linearization is assumed to be valid within an energy range D around the Fermi level. The Q integrals appearing in Eq. (26) can now be written as

$$\int^{K_{F-}} \frac{dQ}{Q - p'_-} = \int_{-D}^{0} \frac{d\epsilon}{\epsilon - \epsilon'},$$

$$\int^{K_{F+}} \frac{dQ}{Q - p'} = \int_{-D}^{0} \frac{d\epsilon}{\epsilon - \epsilon'},$$

$$\int^{K_{F\mp}} \frac{dQ}{Q + Q_\pm - p' - p'_-} = \frac{v_{F\pm}}{v_{F+} + v_{F-}} \int_{-D}^{0} \frac{d\epsilon}{\epsilon - \epsilon'}.$$

The scattering amplitudes with $\uparrow$ ($\downarrow$) spin index are always associated with the momentum p' (p'_-). Therefore, we shall henceforth omit the momentum argument p' (p'_-) of the scattering amplitudes. The divergent perturbative correction, $\delta t_{\uparrow}$, is proportional to $\ln(|\epsilon'|/D)$,

$$\frac{\delta t_{\uparrow}}{\ln\frac{|\epsilon'|}{D}} = \frac{(g_{2\downarrow}-g_{1\downarrow})}{4hv_{F-}} r_{\downarrow}^{*} r_{\downarrow} t_{\uparrow} + \frac{(g_{2\uparrow}-g_{1\uparrow})}{4hv_{F+}} r_{\uparrow}^{*} r_{\uparrow} t_{\uparrow} + \frac{(g_{2\uparrow}-g_{1\uparrow})}{4hv_{F+}} r_{\uparrow}^{*} r_{\uparrow}' t_{\uparrow}' + \frac{(g_{2\downarrow}-g_{1\downarrow})}{4hv_{F-}} r_{\downarrow}^{*} r_{\uparrow}' t_{\downarrow}' + \frac{g_{2\perp}}{2h(v_{F+}+v_{F-})} (r_{\downarrow}'^{*} r_{\uparrow}' t_{\uparrow} + r_{\uparrow}'^{*} r_{\downarrow} t_{\uparrow}' + r_{\uparrow}'^{*} r_{\uparrow} t_{\downarrow}' + r_{\downarrow}'^{*} r_{\uparrow}' t_{\uparrow}). \tag{29}$$

For the calculation of $\delta t_{\uparrow}'(p')$ and $\delta t_{\downarrow}(p_{-}')$, the propagators we need to consider are $-\langle T_{\tau} \hat{a}_{p,\downarrow}(\tau) \hat{c}_{p',\uparrow}^{\dagger} \rangle$ and $-\langle T_{\tau} \hat{a}_{p,\downarrow}(\tau) \hat{c}_{p_{-}',\downarrow}^{\dagger} \rangle$, respectively. The perturbation theory is analogous to that described above. In order to obtain $t_{\downarrow}'(p_{-}')$ we consider the propagator $-\langle T_{\tau} \hat{a}_{p,\uparrow}(\tau) \hat{c}_{p_{-}',\downarrow}^{\dagger} \rangle$.

The logarithmically divergent perturbative terms can be dealt with using a renormalization procedure: we reduce the bandwidth D by removing states in a narrow strip δD near the band edge and work again the perturbation theory in the new bandwidth $D-\delta D$. The effect of removal of the band edge states must be compensated by adopting a new value of $t_{\uparrow}$ for the new bandwidth. Applying this procedure step by step yields successive renormalizations of $t_{\uparrow}$. A differential equation is obtained by noting that the perturbation theory result, $t_{\uparrow}+\delta t_{\uparrow}$, remains invariant as D is reduced,

$$dt_{\uparrow} + \frac{\partial \delta t_{\uparrow}}{\partial D} dD = 0.$$

We introduce now a variable $\xi = \ln(D/D_0)$ which will be integrated from 0 to $\ln(|\epsilon'|/D_0)$, corresponding to the fact that the bandwidth is progressively reduced from D_0 to $|\epsilon'|$ (which will eventually be taken as temperature: $|\epsilon'| = T$) and the scaling differential equations for the transmission amplitudes become

$$\frac{dt_{\uparrow}}{d\xi} = \frac{(g_{2\downarrow}-g_{1\downarrow})}{4hv_{F-}} (r_{\downarrow}^{*} r_{\downarrow} t_{\uparrow} + r_{\downarrow}^{*} r_{\uparrow}' t_{\downarrow}') + \frac{(g_{2\uparrow}-g_{1\uparrow})}{4hv_{F+}} (r_{\uparrow}^{*} r_{\uparrow} t_{\uparrow} + r_{\uparrow}^{*} r_{\uparrow}' t_{\uparrow}') + \frac{g_{2\perp}}{2h(v_{F+}+v_{F-})} (r_{\downarrow}'^{*} r_{\uparrow}' t_{\uparrow} + r_{\uparrow}'^{*} r_{\downarrow} t_{\uparrow}' + r_{\uparrow}'^{*} r_{\uparrow} t_{\downarrow}' + r_{\downarrow}'^{*} r_{\uparrow}' t_{\uparrow}), \tag{30}$$

$$\frac{dt_{\uparrow}'}{d\xi} = \frac{(g_{2\downarrow}-g_{1\downarrow})}{2hv_{F-}} r_{\downarrow}^{*} r_{\downarrow}' t_{\uparrow} + \frac{(g_{2\uparrow}-g_{1\uparrow})}{2hv_{F+}} r_{\uparrow}^{*} r_{\uparrow} t_{\uparrow}' + \frac{g_{2\perp}}{h(v_{F+}+v_{F-})} (r_{\downarrow}'^{*} r_{\uparrow} t_{\uparrow} + r_{\uparrow}'^{*} r_{\downarrow}' t_{\uparrow}'), \tag{31}$$

$$\frac{dt_{\downarrow}}{d\xi} = \frac{(g_{2\uparrow}-g_{1\uparrow})}{4hv_{F+}} (r_{\uparrow}^{*} r_{\uparrow} t_{\downarrow} + r_{\uparrow}^{*} r_{\downarrow}' t_{\uparrow}') + \frac{(g_{2\downarrow}-g_{1\downarrow})}{4hv_{F-}} (r_{\downarrow}^{*} r_{\downarrow} t_{\downarrow} + r_{\downarrow}^{*} r_{\downarrow}' t_{\downarrow}') + \frac{g_{2\perp}}{2h(v_{F+}+v_{F-})} (r_{\uparrow}'^{*} r_{\downarrow}' t_{\downarrow} + r_{\downarrow}'^{*} r_{\uparrow} t_{\downarrow}' + r_{\downarrow}'^{*} r_{\downarrow} t_{\uparrow}' + r_{\uparrow}'^{*} r_{\downarrow}' t_{\downarrow}), \tag{32}$$

$$\frac{dt_{\downarrow}'}{d\xi} = \frac{(g_{2\uparrow}-g_{1\uparrow})}{2hv_{F+}} r_{\uparrow}^{*} r_{\uparrow}' t_{\downarrow} + \frac{(g_{2\downarrow}-g_{1\downarrow})}{2hv_{F-}} r_{\downarrow}^{*} r_{\downarrow} t_{\downarrow}' + \frac{g_{2\perp}}{h(v_{F+}+v_{F-})} (r_{\uparrow}'^{*} r_{\downarrow} t_{\downarrow} + r_{\downarrow}'^{*} r_{\uparrow}' t_{\downarrow}'). \tag{33}$$

In order to obtain the perturbative correction to the reflection amplitude $r_{\uparrow}(p')$ we consider the propagator

$$\mathcal{G}(\tau) = -\langle T_{\tau} \hat{b}_{p,\uparrow}(\tau) \hat{c}_{p',\uparrow}^{\dagger} \rangle \Rightarrow$$

$$\mathcal{G}^{(0)}(i\omega) = \frac{1}{i\omega - \epsilon(p',\uparrow)} \frac{ir_{\uparrow}(p')}{p+p'+i0}. \tag{34}$$

In this case, there is a process where the incoming electron from the left is reflected back by the Hartree potential without even crossing the domain wall. The corresponding term comes from the Wick pairing term

$$\langle \hat{b}_{p,\uparrow}(\tau) \hat{b}_{k_2,\uparrow}^{\dagger}(\tau') \rangle \langle \hat{a}_{k_1,\uparrow}^{\dagger}(\tau') \hat{b}_{k_1-q,\uparrow}(\tau') \rangle \langle \hat{a}_{k_2+q,\uparrow}(\tau') \hat{c}_{p',\uparrow}^{\dagger} \rangle$$

and gives a contribution to $\delta r_{\uparrow}(p')$ equal to

$$\frac{g_{2\uparrow}-g_{1\uparrow}}{4hv_{F+}} r_{\uparrow}(p') \ln\frac{|\epsilon'|}{D}.$$

The differential equation for $r_{\uparrow}(p')$ is

$$\frac{dr_{\uparrow}}{d\xi} = \frac{g_{2\uparrow}-g_{1\uparrow}}{4hv_{F+}} (r_{\uparrow}^{*} r_{\uparrow} r_{\uparrow} + r_{\uparrow}^{*} t_{\uparrow}' t_{\uparrow}') + \frac{g_{2\downarrow}-g_{1\downarrow}}{4hv_{F-}} (r_{\downarrow}^{*} t_{\uparrow} t_{\downarrow} + r_{\downarrow}^{*} r_{\downarrow}' r_{\uparrow}') - \frac{g_{2\uparrow}-g_{1\uparrow}}{4hv_{F+}} r_{\uparrow} + \frac{g_{2\perp}}{2h(v_{F+}+v_{F-})} (r_{\uparrow}'^{*} r_{\downarrow}' r_{\uparrow} + r_{\downarrow}'^{*} r_{\uparrow}' r_{\uparrow} + r_{\uparrow}'^{*} t_{\downarrow} t_{\uparrow}' + r_{\downarrow}'^{*} t_{\uparrow} t_{\uparrow}'), \tag{35}$$

and the differential equation for $r_{\uparrow}'(p')$ is

$$\frac{dr_{\uparrow}'}{d\xi} = \frac{g_{2\uparrow}-g_{1\uparrow}}{4hv_{F+}} (r_{\uparrow}^{*} r_{\uparrow} r_{\uparrow}' + r_{\uparrow}^{*} t_{\uparrow}' t_{\uparrow}) + \frac{g_{2\downarrow}-g_{1\downarrow}}{4hv_{F-}} (r_{\downarrow}^{*} t_{\downarrow} t_{\downarrow}' + r_{\downarrow}^{*} r_{\downarrow} r_{\uparrow}') + \frac{g_{2\perp}}{2h(v_{F+}+v_{F-})} (r_{\uparrow}'^{*} r_{\downarrow} r_{\uparrow} + r_{\downarrow}'^{*} r_{\uparrow}' r_{\uparrow}' + r_{\uparrow}'^{*} t_{\downarrow}' t_{\uparrow}' + r_{\downarrow}'^{*} t_{\uparrow} t_{\uparrow}) - \frac{g_{2\perp}}{2h(v_{F+}+v_{F-})} r_{\uparrow}'. \tag{36}$$

IV. FIXED POINTS

The parameters of the model, which enter the scaling equations, are

$$\frac{g_{2\uparrow}-g_{1\uparrow}}{4hv_{F+}} = g_{\uparrow}, \tag{37}$$

$$\frac{g_{2\downarrow}-g_{1\downarrow}}{4hv_{F-}} = g_{\downarrow}, \tag{38}$$

$$\frac{g_{2\perp}}{2h(v_{F+}+v_{F-})}=g_\perp, \tag{39}$$

and the ratio v_{F-}/v_{F+}. The results can be presented in terms of the transmission coefficients, defined by

$$\mathcal{T}_\uparrow=\frac{v_{F-}}{v_{F+}}|t_\uparrow|^2, \tag{40}$$

$$\mathcal{T}'_\uparrow=|t'_\uparrow|^2, \tag{41}$$

$$\mathcal{T}'_\downarrow=|t'_\downarrow|^2, \tag{42}$$

and the reflection coefficients

$$\mathcal{R}_\uparrow=|r_\uparrow|^2, \tag{43}$$

$$\mathcal{R}_\downarrow=|r_\downarrow|^2, \tag{44}$$

$$\mathcal{R}'_\uparrow=\frac{v_{F-}}{v_{F+}}|r'_\uparrow|^2. \tag{45}$$

By definition, these coefficients refer to the respective currents divided by the incident current.

A. Insulator fixed points

We have made a numerical study of the scaling equations. The noninteracting domain wall described in Sec. II provides the initial scattering parameters for our numerical scaling. Below we describe analytically the scaling behavior close to the fixed points we have found.

For repulsive interactions $(g_\uparrow,g_\downarrow,g_\perp>0)$ the system flows to insulator fixed points. For a moderate to large λ/v_{F+} (larger than about 0.1) all the transmission amplitudes, t_σ and t'_σ, vanish faster than any reflection amplitude as $T\to 0$. We may then rewrite the scaling equations neglecting the small transmission amplitudes. The scaling equation for $r_\uparrow$, for instance, becomes

$$\frac{dr_\uparrow}{d\xi}=g_\uparrow(|r_\uparrow|^2-1)r_\uparrow+g_\downarrow r_\downarrow^* r'_\downarrow r'_\uparrow+2g_\perp\frac{v_{F-}}{v_{F+}}|r'_\uparrow|^2 r_\uparrow, \tag{46}$$

where we used Eq. (A10). The Wronskian relation (A6), allowing for complex reflection amplitudes, shows that

$$r_\downarrow^* r'_\downarrow+r_\uparrow r'^*_\downarrow=0. \tag{47}$$

The charge conservation condition is satisfied solely by the reflections,

$$1=|r_\uparrow|^2+\frac{v_{F-}}{v_{F+}}|r'_\uparrow|^2=|r_\downarrow|^2+\frac{v_{F-}}{v_{F+}}|r'_\uparrow|^2, \tag{48}$$

from which we easily conclude that $|r_\uparrow|=|r_\downarrow|$ at the fixed point. Then, Eq. (46) may be rewritten as

$$\begin{aligned}\frac{dr_\uparrow}{d\xi}&=\frac{v_{F-}}{v_{F+}}(2g_\perp-g_\uparrow-g_\downarrow)|r'_\uparrow|^2 r_\uparrow\\&=\frac{v_{F-}}{v_{F+}}(2g_\perp-g_\uparrow-g_\downarrow)(1-|r_\uparrow|^2)r_\uparrow.\end{aligned} \tag{49}$$

Consider now the scaling equation (36). For $r'_\uparrow$ in case of negligible transmissions we have

$$\frac{dr'_\uparrow}{d\xi}=g_\uparrow|r_\uparrow|^2 r'_\uparrow+g_\downarrow|r_\downarrow|^2 r'_\uparrow+g_\perp\left(r'^*_\uparrow r_\downarrow r_\uparrow+\frac{v_{F-}}{v_{F+}}|r'_\uparrow|^2 r'_\uparrow-r'_\uparrow\right). \tag{50}$$

The Wronskian relation (A6), allowing for complex reflection amplitudes, tells us that

$$r_\downarrow r'^*_\uparrow+\frac{v_{F-}}{v_{F+}}r_\uparrow^* r'_\downarrow=0, \tag{51}$$

and we recast Eq. (50) as

$$\frac{dr'_\uparrow}{d\xi}=(g_\uparrow+g_\downarrow-2g_\perp)\left(1-\frac{v_{F-}}{v_{F+}}|r'_\uparrow|^2\right)r'_\uparrow. \tag{52}$$

In the derivation of (49) and (52) the only assumption made was that the transmission amplitudes are negligibly small. The reflection amplitudes may be, in general, complex and are still renormalized after the transmissions became negligible.

Now we see that Eqs. (49) and (52) predict that the phases of the complex numbers $r_\uparrow$, $r'_\uparrow$ are unchanged during scaling. The two fixed points we may consider correspond to $r_\uparrow$ approaching 0, or $|r_\uparrow|$ approaching 1 along a constant phase line in the complex plane.

The situation $|r_\uparrow|\to 0$ requires $2g_\perp-g_\uparrow-g_\downarrow>0$ and, by charge conservation we have $|r'_\uparrow|\to\sqrt{v_{F+}/v_{F-}}$. Upon integrating (52) with ξ ranging from 0 to $\ln(T/D_0)$, the amplitude $r'_\uparrow$ will vary from its initial value $r'_{\uparrow,0}$ to $r'_\uparrow(T)$. Using the definition (45) for the reflection coefficient, we write

$$\mathcal{R}'_\uparrow(T)=\frac{\dfrac{\mathcal{R}'_{\uparrow,0}}{1-\mathcal{R}'_{\uparrow,0}}\left(\dfrac{T}{D_0}\right)^{2(g_\uparrow+g_\downarrow-2g_\perp)}}{1+\dfrac{\mathcal{R}'_{\uparrow,0}}{1-\mathcal{R}'_{\uparrow,0}}\left(\dfrac{T}{D_0}\right)^{2(g_\uparrow+g_\downarrow-2g_\perp)}}. \tag{53}$$

If $2g_\perp-g_\uparrow-g_\downarrow>0$, then $\mathcal{R}'_\uparrow(T)\to 1$ as $T\to 0$. The domain wall becomes insulating. It reflects all incident electrons while reversing their spin. Therefore, such a DW may be considered as a perfect spin-flip reflector at zero temperature. In order to find the low T behavior of transmissions we set $r_\uparrow=r_\downarrow=0$ in Eqs. (30)–(33) and obtain

$$|t_\uparrow|\sim|t'_\uparrow|\sim|t'_\downarrow|\sim T^{2g_\perp}. \tag{54}$$

Figure 3 shows numerical solutions to the scaling equations, where the system is flowing to this fixed point.

In the regime where $g_\uparrow+g_\downarrow-2g_\perp>0$ we have $\mathcal{R}'_\uparrow(T)\to 0$, $\mathcal{R}_\uparrow(T)\to 1$. So, the domain wall reflects all incident electrons while preserving their spin. From Eqs. (30)–(33) for the transmission amplitudes we obtain

$$\begin{aligned}|t_\uparrow|&\sim T^{g_\uparrow+g_\downarrow},\\|t'_\uparrow|&\sim T^{2g_\uparrow},\\|t'_\downarrow|&\sim T^{2g_\downarrow}.\end{aligned} \tag{55}$$

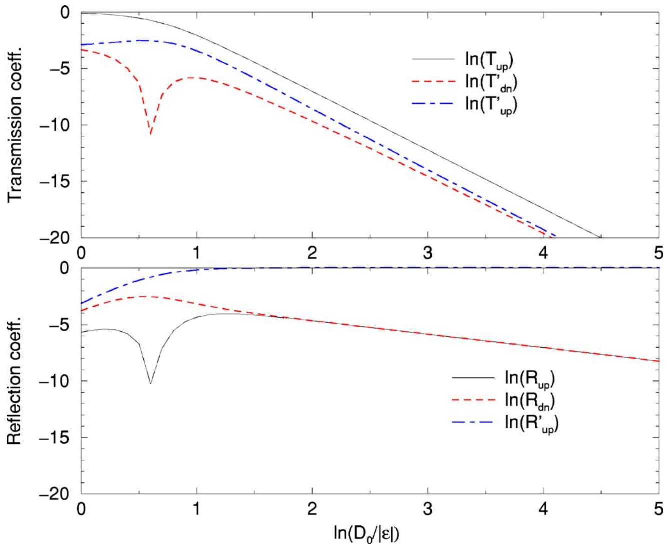

FIG. 3. (Color online) Logarithm of transmission and/or reflection coefficients versus $\ln \frac{D_0}{|\epsilon|}$. We may identify temperature T with $|\epsilon|$. The interaction parameters are $g_\uparrow = g_\downarrow = 1$, $g_\perp = 1.3$ and the noninteracting domain wall model parameters are $V=0$, $v_{F-}/v_{F+} = 0.8$, $v_{F+} = 1$, $\lambda = 0.2$. The dips are due to the sign reversal of the (small) scattering amplitudes. The long linear tails are analytically described in the text. At low temperature the system becomes a 100% spin-flip reflector.

If $g_\uparrow + g_\downarrow - 2g_\perp = 0$ then both $\mathcal{R}'_\uparrow(\mathcal{T})$ and $\mathcal{R}_\uparrow(\mathcal{T})$ tend to finite values. Such a regime is illustrated in Fig. 4. In this case, Eqs. (30), (31), and (33) with constant reflection amplitudes become a linear (in $t_\uparrow$, $t'_\uparrow$, $t'_\downarrow$) algebraic 3×3 system. The eigenvalues of the matrix give three temperature exponents and each transmission amplitude will be a linear combination of the three powers of T. For decreasing temperature, there may be a crossover from one exponent to the other and the lowest exponent dominates as $T \to 0$.

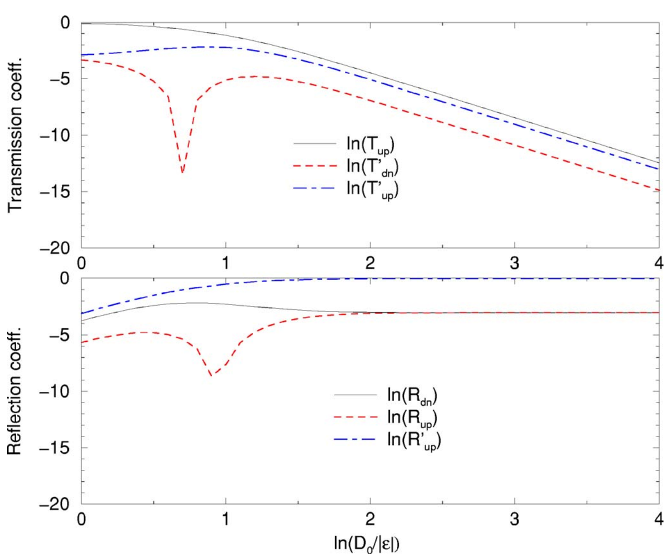

FIG. 4. (Color online) Logarithm of the transmission and/or reflection coefficients versus $\ln(D_0/|\epsilon|)$. We may identify temperature T with $|\epsilon|$. The parameters are $V=0$, $(v_{F-}/v_{F+}) = 0.8$, $g_\uparrow = g_\downarrow = g_\perp = 1$, $v_{F+} = 1$, $\lambda = 0.2$. The reflection coefficients are all finite as $T \to 0$.

For smaller values of λ / v_{F+} (smaller than about 0.1) in the Hamiltonian (1), the system flows to a fixed point, where $r'_\uparrow$ vanishes faster than the transmissions and $|r_\sigma| \to 1$. The transmission amplitudes still scale to zero as in Eqs. (55). The scaling equation (36) for $r'_\uparrow$ can be linearized in $r'_\uparrow$ by neglecting the second order terms in t, t', and considering that $|r_\sigma| \to 1$,

$$\frac{dr'_\uparrow}{d\xi} = (g_\uparrow + g_\downarrow) r'_\uparrow, \tag{56}$$

from which we obtain

$$|\mathcal{R}'_\uparrow| \sim \mathcal{T}^{2(g_\uparrow + g_\downarrow)}. \tag{57}$$

We see that the exponent for $|r'_\uparrow(T)|$ is not bigger than the exponents in (55). Now, in the scaling equation (35) for $r_\uparrow$ we cannot neglect the terms containing transmission amplitudes on the right-hand side. One can easily see that the $g_\uparrow$ term becomes $g_\uparrow(|r_\uparrow|^2 - 1) r_\uparrow$, which is of the same order of magnitude as the other terms. Consequently, the scaling behavior derived in Eqs. (49) and (52) does not apply here, since it was assumed there that the transmissions were smaller than r'_σ. The behavior of r_σ as $T \to 0$ can be found from the charge conservation condition, $\mathcal{R}_\uparrow = 1 - \mathcal{R}'_\uparrow - \mathcal{T}_\uparrow - \mathcal{T}'_\uparrow$, so $1 - \mathcal{R}_\uparrow \sim \mathcal{T}^{\min\{2(g_\uparrow + g_\downarrow), 4g_\uparrow\}}$. Such a situation is shown in Fig. 5, where $t'_\downarrow$ is seen to initially flow very fast to zero. The explanation is the following: for small λ in Eqs. (7) and (8), the noninteracting domain wall has $t_\uparrow > 1$, $r_\uparrow > 0$, and $t_\downarrow < 1$, $r_\downarrow < 0$. Also $t' = r'$ is small. The scaling equation for $t'_\downarrow$ becomes

$$\frac{dt'_\downarrow}{d\xi} = (2g_\uparrow r_\uparrow + 2g_\perp |r_\downarrow|) r'_\downarrow t_\uparrow + (2g_\uparrow r_\downarrow^2 - 2g_\perp |r'_\uparrow r'_\downarrow|) t'_\downarrow.$$

The first term on the right-hand side is positive and much larger than the second one, so $t'_\downarrow$ tends fast to zero and disappears from the equations. The equation for $t'_\uparrow$ is

$$\frac{dt'_\uparrow}{d\xi} = (2g_\downarrow r_\downarrow - 2g_\perp r_\uparrow) r_\downarrow t_\uparrow + (2g_\uparrow r_\uparrow^2 + 2g_\perp |r'_\uparrow r'_\downarrow|) t'_\uparrow.$$

The first term on the right-hand side is negative while the second is smaller because of small initial $t'_\uparrow$. Then, $t'_\uparrow$ initially grows as can be seen in Fig. 5.

B. Transparent barrier fixed points

Zero temperature fixed points corresponding to a transparent domain wall can be achieved when the interaction constants are all negative, i.e., for attractive electron interaction. Although we do not expect such a situation to occur in realistic physical systems, we describe below the fixed points for the case $V=0$ in the model Hamiltonian (1). For moderate to strong λ / v_{F+} in the model (7) and (8), the zero temperature values $1 \geq |t'_\uparrow| = |t'_\downarrow| > |t_\uparrow|$ depend on the initial parameters. Smaller λ / v_{F+} enhances $t_\uparrow$ relative to t'_σ. The reflection coefficients vanish under scaling as powers of temperature. The corresponding exponents can be obtained after linearizing

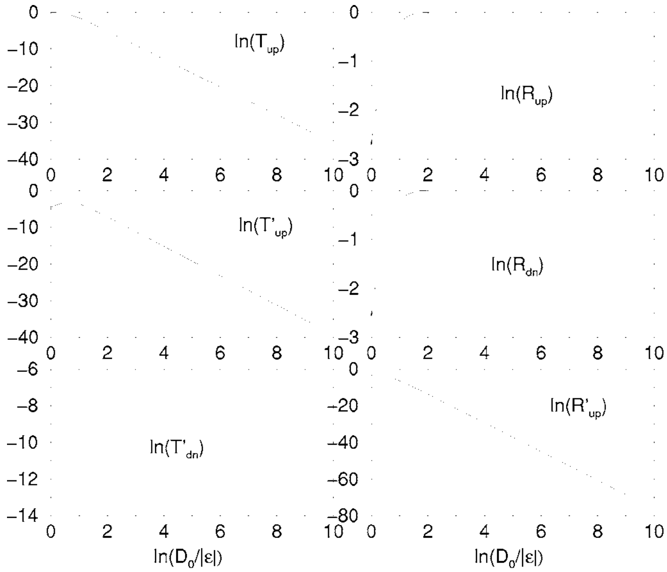

FIG. 5. Logarithm of transmission and/or reflection coefficients versus $\ln(D_0/|\epsilon|)$. We may identify temperature T with $|\epsilon|$. Parameters are $g_\uparrow=1$, $g_\downarrow=0.9$, $g_\perp=1.3$, and $v_{F-}/v_{F+}=0.8$. For the initial noninteracting scattering amplitudes we used $V=0$, $v_{F+}=1$, $\lambda=0.05$.

(for small reflections) the scaling equations (35) and (36). The resulting 3×3 matrix contains the finite limiting values of the transmission amplitudes and its eigenvalues give the temperature exponents for the vanishing reflection amplitudes. Figure 6 shows an example of this behavior.

If some of the interaction constants are positive and the others negative, the situation becomes more complex. Below we describe several possible situations.

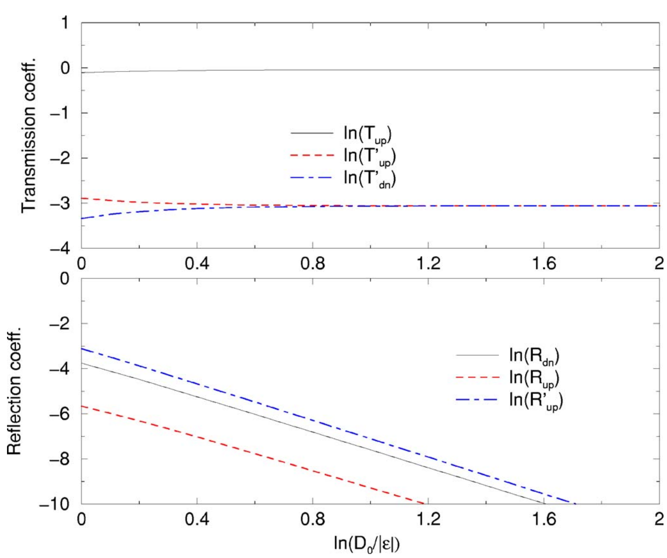

FIG. 6. (Color online) Logarithm of transmission and/or reflection coefficients versus $\ln(D_0/|\epsilon|)$. Parameters are $g_\uparrow=-0.7$, $g_\downarrow=-1.1$, $g_\perp=-1$, and $v_{F-}/v_{F+}=0.8$. For the initial noninteracting scattering amplitudes we used $V=0$, $v_{F+}=1$, $\lambda=0.2$. The transmission coefficients are all finite as $T\to0$.

1. The case $g_\uparrow$, $g_\downarrow>0$, $g_\perp<0$

The system flows to the fixed point $r_\uparrow=r_\downarrow=-1$ with all other amplitudes vanishing. The low-T behavior of the transmission can be easily found by inserting the fixed point reflections into Eqs. (30)–(33),

$$|t_\uparrow|\sim T^{g_\uparrow+g_\downarrow},\quad |t'_\uparrow|\sim T^{2g_\uparrow},\quad |t'_\downarrow|\sim T^{2g_\downarrow}. \tag{58}$$

The scaling equation for $r'_\uparrow$, neglecting second order terms in the scattering amplitudes, takes the form

$$\frac{dr'_\uparrow}{d\xi}=(g_\uparrow+g_\downarrow-2g_\perp)r'_\uparrow\Rightarrow r'_\uparrow\sim T^{g_\uparrow+g_\downarrow-2g_\perp}, \tag{59}$$

so that we must have $g_\uparrow+g_\downarrow-2g_\perp>0$ in order for $r'_\uparrow\to0$.

2. The case $g_\uparrow$, $g_\downarrow<0$, $g_\perp>0$

The system flows to the perfect spin-flip reflector fixed point $|r'_\uparrow|=\sqrt{v_{F+}/v_{F-}}$ with all other amplitudes vanishing, in accordance with the condition $g_\uparrow+g_\downarrow-2g_\perp<0$ derived earlier.

3. The case $g_\uparrow>0$, $g_\downarrow<0$

For a negative or small positive $g_\perp$, the system flows to a fixed point where $|t'_\downarrow|=1$, $r_\uparrow=-1$. The wall transmits all spin-$\downarrow$ particles with a spin-flip and reflects all spin-$\uparrow$ particles. From Eqs. (30)–(33) we see that the exponents for the transmission amplitudes are

$$|t_\uparrow|\sim T^{g_\uparrow},\quad |t'_\uparrow|\sim T^{2g_\uparrow}. \tag{60}$$

After linearizing Eq. (36) for $r'_\uparrow$ in small amplitudes, we have

$$\frac{dr'_\uparrow}{d\xi}\approx(g_\uparrow-g_\perp)r'_\uparrow\Rightarrow r'_\uparrow\sim T^{g_\uparrow-g_\perp}, \tag{61}$$

which requires $g_\uparrow>g_\perp$ for vanishing $r'_\uparrow$. If $g_\uparrow-g_\perp$ is small, the small quantities neglected in the right-hand side of Eq. (61) become important. Therefore, this fixed point holds for $g_\uparrow-g_\perp$ above some small quantity. Linearizing Eq. (34) for $r_\uparrow$ in small amplitudes, we find

$$\frac{dr_\downarrow}{d\xi}\approx-g_\downarrow r_\downarrow^*-g_\downarrow r_\downarrow\Rightarrow r_\downarrow\sim T^{-2g_\downarrow}, \tag{62}$$

which tends to zero since $g_\downarrow<0$. For larger $g_\perp$ the system flows to the spin-flip reflector fixed point ($|r'_\uparrow|\to\sqrt{v_{F+}/v_{F-}}$).

4. The case $g_\uparrow<0$, $g_\downarrow>0$

The situation is analogous to the previous one. For negative or small positive $g_\perp$ the system flows to a fixed point where $|t'_\uparrow|=1$, $r_\downarrow=-1$ with all the others vanishing. The wall transmits all spin-$\uparrow$ particles with a flip and reflects all spin-$\downarrow$ particles. From Eqs. (30)–(33) we see that the exponents for the transmission amplitudes are

$$|t_\uparrow|\sim T^{g_\downarrow},\quad |t'_\downarrow|\sim T^{2g_\downarrow}. \tag{63}$$

Linearizing Eq. (36) for $r'_\uparrow$ in small amplitudes, we have

$$\frac{dr'_\uparrow}{d\xi} \approx (g_\downarrow - g_\perp) r'_\uparrow \Rightarrow r'_\uparrow \sim T^{g_\downarrow - g_\perp}, \tag{64}$$

which requires $g_\downarrow > g_\perp$ in order for $r'_\uparrow$ to vanish. If $g_\downarrow - g_\perp$ is small, the small quantities neglected in the right-hand side of Eq. (64) will become important. Therefore, this fixed point holds for $g_\downarrow - g_\perp$ above some small quantity. For larger $g_\perp$ the system flows to the spin-flip reflector fixed point ($|r'_\uparrow| \to \sqrt{v_{F+}/v_{F-}}$).

V. DISCUSSION AND SUMMARY

Lateral ferromagnetic semiconductor wires with nanoconstrictions make it possible to achieve the limit of sharp domain walls.[25] It has been shown that the constriction itself does not cause significant reflection of the incident waves because it only produces a semiclassical potential.[46] We may estimate the parameter λ of our model (1) by assuming that $\vec{M}(z) = M_0 \cos\theta(z)\hat{z} + M_0 \sin\theta(z)\hat{x}$ with $\cos\theta(z) = \tanh(z/L)$,[38] where L is the width of the domain wall. We then find

$$\lambda = \frac{JM_0}{\hbar} \int_{-\infty}^{\infty} \sin\theta(z) dz = \pi \frac{JM_0}{\hbar} L, \tag{65}$$

implying that

$$\frac{\lambda}{v_{F+}} = \pi \frac{JM_0}{(\hbar^2 k_{F+}^2/m)} (Lk_{F+}). \tag{66}$$

The condition for the domain wall to be smaller than the Fermi wavelength is $Lk_{F+} < 2\pi$. The smaller Fermi wavelength is that of majority spin electrons, k_{F+}. On the other hand, for small Lk_{F+} the barrier becomes a poor spin-flip scatterer. The ratio v_{F-}/v_{F+} depends on the polarization degree of the electron system. We consider now a one-channel system. In a nonmagnetic system there is a single Fermi momentum k_F for up and down electrons, and the Fermi energy is $E_F = \hbar^2 k_F^2/(2m)$. Once the system becomes magnetized, the two new Fermi momenta, $k_{F\pm}$, satisfy the particle conservation condition,

$$k_{F+} + k_{F-} = 2k_F \Rightarrow \frac{k_{F+}}{k_F} + \frac{k_{F-}}{k_F} = 2, \tag{67}$$

and the spin-up and spin-down Fermi surfaces must correspond to the same energy,

$$\frac{\hbar^2 k_{F+}^2}{m} - \frac{\Delta E}{2} = \frac{\hbar^2 k_{F-}^2}{m} + \frac{\Delta E}{2}, \tag{68}$$

where $\Delta E/2 = JM_0$ is the Zeeman shift of the bands. From this we get

$$\frac{k_{F\pm}}{k_F} = 1 \pm \frac{\Delta E}{4E_F}, \tag{69}$$

so that the ratio k_{F-}/k_{F+} is

$$\frac{k_{F-}}{k_{F+}} = \frac{v_{F-}}{v_{F+}} = \frac{1 - (\Delta E/4E_F)}{1 + (\Delta E/4E_F)}. \tag{70}$$

Inserting (69) into Eq. (66) we obtain

$$\frac{\lambda}{v_{F+}} = \pi \frac{(\Delta E/4E_F)}{[1 + (\Delta E/4E_F)]^2} (Lk_+). \tag{71}$$

The full polarization limit is $k_{F-} = 0$ and $k_{F+} = 2k_F$, meaning that $\Delta E/4E_F = 1$, and then Eq. (71) gives

$$\frac{\lambda}{v_{F+}} \approx 0.79 Lk_{F+}.$$

Typical values for a non-fully polarized system are $E_F = 90$ meV and $\Delta E = 30$ meV.[25] In this case we have $v_{F-}/v_{F+} = 0.84$ and Eq. (71) gives

$$\frac{\lambda}{v_{F+}} \approx 0.22 Lk_{F+}.$$

Therefore, if Lk_{F+} is smaller than about 2π, the system can flow to any of the fixed points described above, especially the ones described in Sec. IV A.

The lateral quantization may produce several channels. The higher channels have larger Fermi wavelength and larger $\Delta E/4E_F$, so they can be in the spin-flip reflector fixed point. If a channel of high energy is fully spin polarized, then it corresponds to $\lambda/v_{F+} = 0.79 Lk_{F+}$. But the possibility of interchannel scattering arises. This could be due to the two following reasons: (i) electron-electron interactions (such would require a modification of our theory to allow for interchannel scattering); (ii) the impurity scattering. For the latter to be negligible we need the electron mean free path (*not* the transport mean free path) to be larger than the size of the constriction.

In summary, we have studied the effect of electron-electron interactions on the transmission through a domain wall in a ferromagnetic wire in the regime in which the wall width is smaller than the Fermi wavelength. Applying a renormalization technique to the logarithmically divergent perturbation, we obtained the scaling equations for the scattering amplitudes. The $T=0$ fixed points were identified corresponding to: (i) perfectly insulating wall (with or without complete spin reversal), and (ii) transparent wall. Both repulsive and attractive interactions were considered. We have estimated physical parameters for a domain wall model which may be realized in physical systems. Such estimates suggest that realistic systems can display the behavior predicted in the vicinity of the fixed points we have found.

ACKNOWLEDGMENTS

Discussions with P. A. Lee, A. H. Castro Neto, and P. Sacramento are gratefully acknowledged. M.A.N.A. is grateful to Fundação para a Ciência e Tecnologia for a sabbatical grant. This research was supported by Portuguese program POCI under Grant No. POCI/FIS/58746/2004, EU through RTN Spintronics (Contract No. HPRN-CT-2000-000302), Polish State Committee for Scientific Research under

Grant No. 2 P03B 053 25, by STCU Grant No. 3098 in Ukraine, and by the German DFG under Grant No. SSP 1165, BE216/3-2.

APPENDIX A: GENERALIZATION OF THE WRONSKIAN THEOREM TO SPINOR SCATTERING STATES

The Wronskian theorem[44] for (spin degenerate) scattering states in one-dimensional systems can be easily generalized to spinor states in a spin-dependent scattering potential. Let $\psi_1(z)$ and $\psi_2(z)$ represent two spinor scattering states with energies ϵ_1 and ϵ_2 in the potential $\hat{V}(z)$. We assume $\hat{V}(z)$ to be a 2×2 real symmetric matrix, as is the case in the Hamiltonian (1), and consider a symmetric mass tensor $\hat{m}$ (possibly position and spin dependent). Each spinor satisfies the Schrödinger equation

$$\frac{d}{dz}\frac{1}{\hat{m}}\frac{d\psi_1}{dz}+(\epsilon_1-\hat{V})\psi_1=\begin{pmatrix}0\\0\end{pmatrix}, \tag{A1}$$

$$\frac{d}{dz}\frac{1}{\hat{m}}\frac{d\psi_2}{dz}+(\epsilon_2-\hat{V})\psi_2=\begin{pmatrix}0\\0\end{pmatrix}. \tag{A2}$$

If we multiply the first equation (on the left-hand side) by $\psi_2^t(z)$, the second equation by $\psi_1^t(z)$, and subtract the two, we obtain

$$\frac{d}{dz}\left(\psi_1^t\frac{1}{\hat{m}}\frac{d\psi_2}{dz}-\psi_2^t\frac{1}{\hat{m}}\frac{d\psi_1}{dz}\right)=(\epsilon_1-\epsilon_2)\psi_1^t\psi_2, \tag{A3}$$

where the dot denotes the matrix (spinor) product ($\psi_1^t\psi_2=\Sigma_\sigma\psi_{1,\sigma}\psi_{2,\sigma}$). The expression in large parentheses is a scalar function of z and would be proportional to the Wronskian of the functions ψ_1 and ψ_2^* in the case where the mass tensor reduces to a scalar. If the two states are degenerate ($\epsilon_1=\epsilon_2$), we conclude from (A3) that the expression in large parentheses is independent of the coordinate z,

$$W(\psi_1,\psi_2)\equiv\psi_1^t(z)\frac{1}{\hat{m}}\frac{d\psi_2}{dz}-\psi_2^t(z)\frac{1}{\hat{m}}\frac{d\psi_1}{dz}=\text{const.} \tag{A4}$$

Since the potential matrix $\hat{V}$ is real, then ψ_1^* (or ψ_2^*) also satisfies the Schrödinger equation.

The usefulness of the theorem expressed in Eq. (A4) is that it allows us to establish general relations between the scattering amplitudes, independently of the detailed form of the potential barrier.

If we evaluate (A4) for a pair of degenerate scattering states, say $W(\psi_{k,\uparrow}^*,\psi_{k_-,\downarrow})$, the result must be the same for $z<0$ as for $z>0$,

$$W(\psi_{k,\uparrow}^*,\psi_{k_-,\downarrow})]_{z<0}=W(\psi_{k,\uparrow}^*,\psi_{k_-,\downarrow})]_{z>0}, \tag{A5}$$

which yields

$$v_-t_\uparrow^*(k)t_\downarrow'(k_-)+vt_\uparrow'^*(k)t_\downarrow(k_-)+vr_\uparrow^*(k)r_\downarrow'(k_-)+v_-r_\uparrow'^*(k)r_\downarrow(k_-)=0. \tag{A6}$$

Similarly, calculation of $W(\psi_{k,\uparrow}^*,\psi_{-k_-,\uparrow})$ gives the relation

$$v_-t_\uparrow^*(k)r_\downarrow(k_-)+vt_\uparrow'^*(k)r_\downarrow'(k_-)+vr_\uparrow^*(k)t_\downarrow(k_-)+v_-r_\uparrow'^*(k)t_\downarrow'(k_-)=0, \tag{A7}$$

and $W(\psi_{k,\uparrow}^*,\psi_{-k_-,\downarrow})$ gives the relation

$$v_-t_\uparrow^*(k)r_\uparrow'(k)+vt_\uparrow'^*(k)r_\uparrow(k)+vr_\uparrow^*(k)t_\uparrow'(k)+v_-r_\uparrow'^*(k)t_\uparrow(k)=0. \tag{A8}$$

A fourth relation can be obtained from $W(\psi_{k_-,\downarrow}^*,\psi_{-k_-,\uparrow})$,

$$v_-t_\downarrow'^*(k_-)r_\downarrow(k_-)+vt_\downarrow^*(k_-)r_\downarrow'(k_-)+vr_\downarrow'^*(k_-)t_\downarrow(k_-)+v_-r_\downarrow^*(k_-)t_\downarrow'(k_-)=0. \tag{A9}$$

From $W(\psi_{k,\uparrow},\psi_{k_-,\downarrow})$ we obtain the relation

$$vr_\downarrow'(k_-)=v_-r_\uparrow'(k), \tag{A10}$$

and $W(\psi_{k,\uparrow},\psi_{-k_-,\uparrow})$ gives

$$vt_\downarrow(k_-)=v_-t_\uparrow(k). \tag{A11}$$

Considering a state and its conjugate, $W(\psi_{k,\sigma}^*,\psi_{k,\sigma})$ gives the conservation of the charge current,

$$v=v_-|t_\uparrow|^2+v|t_\uparrow'|^2+v|r_\uparrow|^2+v_-|r_\uparrow'|^2, \tag{A12}$$

for $\sigma=\uparrow$, and

$$v_-=v|t_\downarrow|^2+v_-|t_\downarrow'|^2+v_-|r_\downarrow|^2+v|r_\downarrow'|^2, \tag{A13}$$

for $\sigma=\downarrow$. The results (A6)–(A9), (A12), and (A13) also follow from the unitarity of the S matrix for this scattering problem. One can also regard (A3) as a particular case of the Liouville-Ostrogradski formula.[47]

APPENDIX B: FORMULATION FOR SPIN-DEPENDENT ELECTRON EFFECTIVE MASSES

Electron interactions such as g_4 and g_2, which describe forward scattering between particles moving in the same direction, may produce renormalization of the electron's effective mass.[45] The latter could depend on spin orientation because the Fermi surfaces of spin-up and spin-down electrons are different. These effects can be taken into account from the beginning by rewriting the Hamiltonian (1) in a more general form,

$$\hat{H}_0=-\frac{\hbar^2}{2}\frac{d}{dz}\frac{1}{\hat{m}(z)}\frac{d}{dz}+\hbar V\delta(z)-JM_z(z)\hat{\sigma}_z-\hbar\lambda\delta(z)\hat{\sigma}_x, \tag{B1}$$

where, in the kinetic energy term, we allow for a position and spin-dependent effective mass tensor, $\hat{m}(z)$. The tensor may take the form

$$\hat{m}(z)=\begin{pmatrix}m_\uparrow(z) & 0\\ 0 & m_\downarrow(z)\end{pmatrix}, \tag{B2}$$

with

$$m_{\uparrow}(z) = m_{+}\Theta(-z) + m_{-}\Theta(z)$$

and

$$m_{\downarrow}(z) = m_{-}\Theta(-z) + m_{+}\Theta(z),$$

where $\Theta(z)$ denotes the Heaviside function.

The appropriate mass values must be used in Eqs. (2)–(4). The expressions for the scattering eigenstates and transmission amplitudes given in the main text remain unchanged if we take into account that the velocities must be calculated considering the renormalized masses.

*On leave from Departamento de Física, Universidade de Évora, P-7000-671, Évora, Portugal.

[1] A. Hubert and R. Schäfer, *Magnetic Domains: The Analysis of Magnetic Microstructures* (Springer, Berlin, 1998).
[2] H. X. Tang, S. Masmanidis, R. K. Kawakami, D. D. Awschalom, and M. L. Roukes, Nature (London) **431**, 52 (2004).
[3] J. A. Katine, F. J. Albert, R. A. Buhrman, E. B. Myers, and D. C. Ralph, Phys. Rev. Lett. **84**, 3149 (2000); A. Fert, V. Gros, J. M. George, J. Grollier, H. Jaffrès, A. Hamzic, A. Vaurès, G. Faini, J. Ben Youssef, and H. Le Gall, J. Magn. Magn. Mater. **272-276**, 1706 (2004).
[4] A. Yamaguchi, T. Ono, S. Nasu, K. Miyake, K. Mibu, and T. Shinjo, Phys. Rev. Lett. **92**, 077205 (2004); M. Yamanouchi, D. Chiba, F. Matsukura, and H. Ohno, Nature (London) **428**, 539 (2004); E. Saltoh, H. Miyajima, T. Yamaoka, and G. Tatara, *ibid.* **432**, 203 (2004).
[5] M. Viret *et al.*, Phys. Rev. Lett. **85**, 3962 (2000).
[6] U. Ruediger, J. Yu, S. Zhang, A. D. Kent, and S. S. P. Parkin, Phys. Rev. Lett. **80**, 5639 (1998).
[7] L. Klein *et al.*, Phys. Rev. Lett. **84**, 6090 (2000).
[8] U. Ebels, A. Radulescu, Y. Henry, L. Piraux, and K. Ounadjela, Phys. Rev. Lett. **84**, 983 (2000).
[9] T. Taniyama, I. Nakatani, T. Namikawa, and Y. Yamazaki, Phys. Rev. Lett. **82**, 2780 (1999).
[10] Y. B. Xu, C. A. F. Vaz, A. Hirohata, H. T. Leung, C. C. Yao, J. A. C. Bland, E. Cambril, F. Rousseaux, and H. Launois, Phys. Rev. B **61**, R14901 (2000).
[11] R. Danneau *et al.*, Phys. Rev. Lett. **88**, 157201 (2002).
[12] L. Berger, J. Appl. Phys. **49**, 2156 (1978).
[13] G. G. Cabrera and L. M. Falicov, Phys. Status Solidi B **61**, 539 (1974); **62**, 217 (1974).
[14] M. Viret, D. Vignoles, D. Cole, J. M. D. Coey, W. Allen, D. S. Daniel, and J. F. Gregg, Phys. Rev. B **53**, 8464 (1996).
[15] P. M. Levy and S. Zhang, Phys. Rev. Lett. **79**, 5110 (1997).
[16] G. Tatara and H. Fukuyama, Phys. Rev. Lett. **78**, 3773 (1997).
[17] R. P. van Gorkom, A. Brataas, and G. E. W. Bauer, Phys. Rev. Lett. **83**, 4401 (1999).
[18] P. Bruno, Phys. Rev. Lett. **83**, 2425 (1999).
[19] O. Pietzsch, A. Kubetzka, M. Bode, and R. Wiesendanger, Phys. Rev. Lett. **84**, 5212 (2000).
[20] K. Miyake *et al.*, J. Appl. Phys. **91**, 3468 (2002).
[21] M. Kläui, C. A. F. Vaz, J. Rothman, J. A. C. Bland, W. Wernsdorfor, G. Faini, and E. Combril, Phys. Rev. Lett. **90**, 097202 (2003).
[22] S. A. Wolf *et al.*, Science **294**, 1488 (2001).
[23] N. García, M. Muñoz, and Y. W. Zhao, Phys. Rev. Lett. **82**, 2923 (1999); G. Tatara, Y. W. Zhao, M. Muñoz, and N. García, *ibid.* **83**, 2030 (1999).
[24] H. D. Chopra and S. Z. Hua, Phys. Rev. B **66**, 020403(R) (2002); S. Z. Hua and H. D. Chopra, *ibid.* **67**, 060401(R) (2003).
[25] C. Rüster, T. Borzenko, C. Gould, G. Schmidt, L. W. Molenkamp, X. Liu, T. J. Wojtowicz, J. K. Furdyna, Z. G. Yu, and M. E. Flatté, Phys. Rev. Lett. **91**, 216602 (2003).
[26] L. R. Tagirov, B. P. Vodopyanov, and K. B. Efetov, Phys. Rev. B **65**, 214419 (2002); **63**, 104428 (2001).
[27] J. B. A. N. van Hoof, K. M. Schep, A. Brataas, G. E. W. Bauer, and P. J. Kelly, Phys. Rev. B **59**, 138 (1999).
[28] J. Kudrnovský, V. Drchal, C. Blaas, P. Weinberger, I. Turek, and P. Bruno, Phys. Rev. B **62**, 15084 (2000); J. Kudrnovský, V. Drchal, I. Turek, P. Středa, and P. Bruno, Surf. Sci. **482-485**, 1107 (2001).
[29] B. Yu. Yavorsky, I. Mertig, A. Ya. Perlov, A. N. Yaresko, and V. N. Antonov, Phys. Rev. B **66**, 174422 (2002).
[30] M. Ye. Zhuravlev, E. Y. Tsymbal, S. S. Jaswal, A. V. Vedyayev, and B. Dieni, Appl. Phys. Lett. **83**, 3534 (2003).
[31] V. K. Dugaev, J. Berakdar, and J. Barnaś, Phys. Rev. B **68**, 104434 (2003); V. K. Dugaev, J. Barnaś, J. Berakdar, V. I. Ivanov, W. Dobrowolski, and V. F. Mitin, Phys. Rev. B **71**, 024430 (2005).
[32] E. Šimanek, Phys. Rev. B **63**, 224412 (2001).
[33] A. O. Gogolin, A. A. Nersesyan, and A. M. Tsvelik, *Bosonization and Strongly Correlated Systems* (Cambridge University Press, Cambridge, 1998).
[34] S. Tomonaga, Prog. Theor. Phys. **5**, 544 (1950).
[35] J. M. Luttinger, J. Math. Phys. **4**, 1154 (1963).
[36] C. L. Kane and M. P. A. Fisher, Phys. Rev. Lett. **68**, 1220 (1992).
[37] C. L. Kane and M. P. A. Fisher, Phys. Rev. B **46**, 7268 (1992).
[38] R. G. Pereira and E. Miranda, Phys. Rev. B **69**, 140402(R) (2004).
[39] T. Hikihara, A. Furusaki, and K. A. Matveev, Phys. Rev. B **72**, 035301 (2005).
[40] K. A. Matveev, Dongxiao Yue, and L. I. Glazman, Phys. Rev. Lett. **71**, 3351 (1993); Dongxiao Yue, L. I. Glazman, and K. A. Matveev, Phys. Rev. B **49**, 1966 (1994).
[41] S. W. Tsai, D. L. Maslov, and L. I. Glazman, Phys. Rev. B **65**, 241102(R) (2002).
[42] P. Devillard, A. Crépieux, K. I. Imura, and T. Martin, Phys. Rev. B **72**, 041309 (2005).
[43] V. K. Dugaev, J. Berakdar, and J. Barnaś, Phys. Rev. B **68**, 104434 (2003).
[44] A. Messiah, *Quantum Mechanics* (North-Holland, Amsterdam, 1999), p. 98.
[45] J. Solyom, Adv. Phys. **28**, 201 (1979).
[46] L. I. Glazman, G. B. Lesovik, D. E. Khmelnitskii, and R. I. Shekhter, Pis'ma Zh. Eksp. Teor. Fiz. **48**, 218 (1988) [JETP Lett. **48**, 239 (1988)].
[47] P. Hartman, *Ordinary Differential Equations* (Birkhäuser, Boston, 1982).